Risk-based Autonomous Maritime Collision Avoidance Considering Obstacle Intentions*

Trym Tengesdal, Tor Arne Johansen and Edmund Brekke

***Abstract*—A robust and efficient Collision Avoidance (COLAV) system for autonomous ships is dependent on a high degree of situational awareness. This includes inference of the intent of nearby obstacles, including compliance with traffic rules such as COLREGS, in order to enable more intelligent decision making for the autonomous agent. Here, a generalized framework for obstacle intent inference is introduced. Different obstacle intentions are then considered in the Probabilistic Scenario-Based Model Predictive Control (PSB-MPC) COLAV algorithm using an examplatory intent model, when statistics about traffic rules compliance and the next waypoint for an obstacle are assumed known. Simulation results show that the resulting COLAV system is able to make safer decisions when utilizing the extra intent information.**

***Index Terms*—Maritime collision avoidance, Autonomous ships, COLREGS, Collision probability, Collision risk, Intention probability, Model predictive control**

I. Introduction

It is estimated that over 75 % of maritime accidents are attributed to human errors [1]–[3]. Thus, there are potential safety gains by introducing autonomously operated ships. The economical and environmental aspects are also positive, as for instance seen by the Yara Birkeland initiative, aiming to replace 40000 yearly truck journeys in Norway [4].

Autonomous ships that operate at sea must rely on a robust COLAV system in order to efficiently avoid nearby obstacles, be it dynamic or static ones. To enable this, a high degree of situational awareness is needed in the system to allow for intelligent choices of avoidance maneuvers that achieve acceptable collision risk while not being overly conservative. Here, information about the intention of nearby obstacles has high value, as it will enable the COLAV system to take more informed and less conservative decisions by considering future trajectories which reflect the current obstacle intention.

Predicting obstacle trajectories and infering their intentions will be a key part of robust deliberate COLAV systems. Different approaches for doing this have been introduced outside the COLAV setting. For COLAV, we are typically interested in the time scale of minutes, and there are different methods employing Automatic Identification System (AIS) data for long-term predictions, as in for instance [5]–[8]. The intent of objects are predicted in [9] using a Bayesian approach, when assuming that a finite set of possible endpoints for their trajectories are known. The method constructs so-called bridge distributions for each possible endpoint, and uses a linear motion model conditioned on the endpoint to reduce the trajectory uncertainty from the current object position to its waypoint. The motion model parameters are learned using historic data.

Considering obstacle intentions in collision free path planning for air traffic and road vehicles has previously been studied [10] [11]. For instance in [11], goal hypotheses of road driving obstacles are formed based on the current road topology, and a probabilistic motion model is used to predict their future trajectories conditioned on the hypotheses. However, for maritime applications, it is to the author's knowledge only [12] and [13] that considers nearby obstacles to be agents capable of different maneuvers or intentions. In [12], an A* search method is applied to collision free path planning which penalizes high collision risk, traffic rule violations and path deviation. An intention motion model is used for nearby civilian vessels, where historical state observations and vessel characteristics are used to output predicted trajectories and classify the vessels as compliant to the International Regulations for Avoiding Collisions at Sea (COLREGS) [14] or not. Information on how this intention model is implemented is limited. The positional uncertainty of an obstacle's predicted trajectory is estimated offline using Monte Carlo Simulation (MCS) for a given scene. The predicted trajectories also incorporate reactive obstacle avoidance for the obstacle to avoid the own-ship and other vessels. In [13], the maneuvering intent of obstacles are estimated using a Kalman Filter (KF). The intents are further used to calculate the collision probability with obstacles by considering reachable sets. A simple COLAV system is then implemented by making evasive maneuvers when the collision probability is above a certain threshold.

In this work, the effect of taking probabilistic information of obstacle intentions into account will be showcased. The novelty lies in introducing a generalized framework for obstacle intention inference and applying this in a COLAV system. The probability of a finite set of obstacle intentions is considered, when the next waypoint of obstacles is assumed known from some source of information in addition to their degree of COLREGS compliance. This can be the case when vessel-to-vessel communication is employed to get waypoint information of nearby vessels or if local traffic pattern analysis is used. A modified version of the Probabilistic Scenario-Based Model Predictive Control (PSB-MPC) [15] is proposed, which

*This work was supported by the Research Council of Norway through the Centers of Excellence funding scheme, project number 223254, Centre for Autonomous Marine Operations and Systems (AMOS), and through the MAROFF funding scheme, project number 295033.

The authors are with AMOS, Department of Engineering Cybernetics, Norwegian University of Science and Technology, 7491 Trondheim, Norway {trym.tengesdal, tor.arne.johansen, edmund.brekke}@ntnu.no

takes obstacle intentions into account through an enhanced prediction scheme using an Ornstein-Uhlenbeck (OU) process as in [16]. The scheme allows obstacles to take different alternative maneuvers at multiple time instants in the horizon. In addition, an updated method of estimating collision probabilities is used in the PSB-MPC, which calculates the collision probability estimates considering piecewise linear segments for the own-ship and obstacle trajectories.

II. Intention Probability Framework

A. Generalized Framework

The index $a = 1, 2, ..., n_a$ is here defined as the obstacle intention. The probability of intention a for obstacle i is denoted $\mathbb{P}_a^i$. The probability is for a finite time interval from t_{k-1} to t_k, where k is the discrete time index, and is assumed to be known as an input to the COLAV system in the form of a conditional probability

$$\mathbb{P}_a^i = \Pr(a|i, \mathcal{I}), \quad \text{where} \quad \sum_{a=1}^{n_a} \mathbb{P}_a^i = 1 \tag{1}$$

In general, the variable $\mathcal{I}$ contains information on all factors that will affect the obstacle intention. Factors such as the type of obstacle, the grounding hazards, nearby static and dynamic obstacles, weather, the obstacle's current state of perception, and its planned route will all affect this probability. A Bayesian network can here be used to represent the dependence of obstacle intentions on these factors. This is illustrated for an example network in Fig. 1. The variable $\mathcal{I}$ is here represented by the seven factors. Note that the network is not unique, and a modelling choice has been made such that intentions are indirectly dependent on for instance the ship type and nearby obstacles through the situation type.

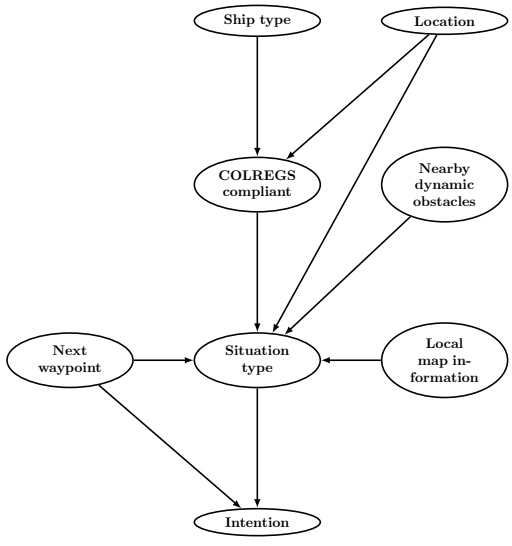

Fig. 1. Example Bayesian net for intention inference for an obstacle ship, considering seven factors (topmost nodes). The situation type is here either overtaking, head-on or crossing, and whether or not the obstacle is stand-on or give-way vessel. Nearby dynamic obstacles can e.g. be represented by a list containing data structures carrying data on their states.

It is a non-trivial task to estimate $\mathbb{P}_a^i$, as the information in $\mathcal{I}$ must be inferred from a subset of all factors involved. Knowledge of this variable is assumed. The purpose of this article is not to show how to infer obstacle intentions, but to demonstrate the potential gain of using probabilistic information about this for decision making in a COLAV system. However, the framework opens up the possibility to use machine learning methods to learn Bayesian nets for obstacle intention inference by for instance employing historic AIS data.

B. A Simple Intention Model

1) Model Assumptions: Three intentions for an obstacle are here considered ($n_a = 3$), corresponding to the obstacle keeping its current course and speed ($a = 1$), taking a starboard ($a = 2$) or port turn ($a = 3$), respectively. It is assumed that the next waypoint WP^i of an obstacle i is known, for instance through vessel-to-vessel communication, and also probabilistic information about its tendency to adhere to COLREGS is known. Then, the situation type (ST) is used to determine the intention probability model used. This is similar to the case in Fig. 1 when only the situation type (ST^i), COLREGS compliance (CC^i), nearby obstacles (including the own-ship) and the next waypoint for obstacle i are considered. Moreover, the situation type is assumed independent on the next obstacle waypoint here.

COLREGS compliance is considered when the distance from the obstacle to the own-ship d_{0i} is less than some threshold d_{close} [17]. The ST^i is formulated as a tuple determining if it is an overtaking (OT), head-on (HO) or crossing (CR) scenario, and whether or not the obstacle is the give-way (GW) or stand-on (SO) vessel. These situations can be determined using the position, heading and velocity of the own-ship and obstacle [17]. For the case when $d_{0i} > d_{close}$, i.e. when the ships are outside the defined COLREGS consideration limit, then $ST^i = \emptyset$. The conditional intention probabilities can then be calculated as

$$\mathbb{P}_a^i = \Pr\{a|\, WP^i, ST^i\} \Pr\{ST^i|CC^i\} \Pr\{CC^i\} \tag{2}$$

An *a priori* COLREGS compliance probability $\Pr\{CC^i\}$ will be used here, but could in general be inferred through knowledge on for instance the obstacle ship type and its current location. The next obstacle waypoint is assumed known, but the route towards this waypoint is uncertain. Further, it is assumed that ST^i can be calculated deterministically given CC^i. Thus, the only unknown probability remaining is $\Pr\{a|\, WP^i, ST^i\}$, which is specified by ad hoc intention models in this article.

Table I summarizes the conditional intention cases given WP^i, ST^i and CC^i. In Table I, the intention is indepedent of the next waypoint for $ST^i = B$ to F, as COLREGS compliance is assumed to have the highest priority. If the obstacle is not CC, then the waypoint dependent intention model will be used, i.e. as for $ST^i = A$. Note that this is weighted by the prior CC probability $\Pr\{CC^i\}$.

TABLE I
CONDITIONAL INTENTION PROBABILITY GIVEN WP^i, ST^i AND INDIRECTLY THROUGH CC^i. THE SITUATION TYPE IS GIVEN SINGLE LETTERS FROM A TO F TO MINIMIZE NOTATION SPACE.

CC^i	ST^i	$\Pr\{a\|WP^i, ST^i\}$
$True$	$A = \emptyset$	$\Pr\{a\|WP^i, A\}$
	$B = (OT, SO)$	$\Pr\{a\|B\}$
	$C = (CR, SO)$	$\Pr\{a\|C\}$
	$D = (OT, GW)$	$\Pr\{a\|D\}$
	$E = (HO, GW)$	$\Pr\{a\|E\}$
	$F = (CR, GW)$	$\Pr\{a\|F\}$
$False$	$A = \emptyset$	$\Pr\{a\|WP^i, A\}$

With the stated assumptions, the intention probability $\mathbb{P}_a^i$ simplifies to

$$\mathbb{P}_a^i = \Pr\{a|\, WP^i, ST^i\}\Pr\{CC^i\} \tag{3}$$

2) Waypoint Dependent Intention: For $ST = A$, we consider the waypoint information, where a simple ad hoc model for the obstacle intention is developed considering the obstacle course χ^i and the Line of Sight (LOS) vector $\boldsymbol{L}^i$ from the obstacle to its next waypoint. This is illustrated for an example head-on scenario in Fig. 2.

The angle θ is defined as the angular difference between the LOS-vector to the waypoint and the obstacle course, and used to define the intention probability of straight line motion, starboard or port maneuvers. The probability for the obstacle to keep its course $a = 1$ is then assumed on the form

$$\Pr\{a = 1|\, WP^i, A\} = \alpha_{1,WP} e^{-c_1|\theta|} + \alpha_{2,WP} \tag{4}$$

where $c_1 > 0$ is a parameter to decide the decrease/increase in probability as the obstacle turns towards the end point. The parameters $\alpha_{1,WP}$ and $\alpha_{2,WP}$ determines the maximum

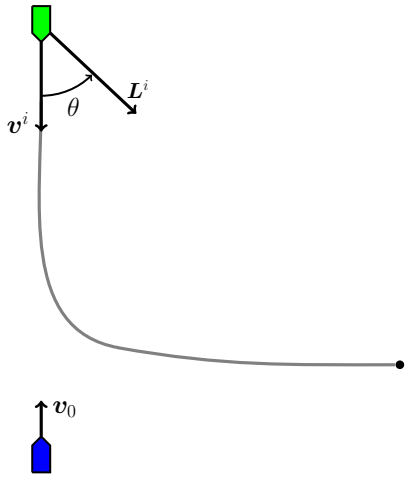

Fig. 2. A head-on scenario with obstacle i in green and own-ship in blue. Their velocity vectors $\boldsymbol{v}^i$ and $\boldsymbol{v}_0$ are also shown. The unknown ground truth planned obstacle path is shown in grey, with its next waypoint assumed known to the own-ship as the black dot.

probability for the waypoint dependent intention a. For a starboard or port maneuver at some time $t_{turn} \geq t_0$, where t_0 is the current time, the intention probabilities are assumed to be

$$\Pr\{a = 2|\, WP^i, A\} = \begin{cases} \alpha_{1,WP}(1 - e^{-c_1\theta}) \\ \quad + \alpha_{2,WP} & \text{if } \theta \geq 0. \\ \alpha_{3,WP}, & \text{otherwise.} \end{cases} \tag{5}$$

$$\Pr\{a = 3|\, WP^i, A\} = \begin{cases} \alpha_{1,WP}(1 - e^{c_1\theta}) \\ \quad + \alpha_{2,WP} & \text{if } \theta \leq 0. \\ \alpha_{3,WP}, & \text{otherwise.} \end{cases} \tag{6}$$

respectively. The weigthing parameters satisfy

$$\alpha_{1,WP} + 2\alpha_{2,WP} + \alpha_{3,WP} = 1 \tag{7}$$

If the probability of a maneuver to a given side is high due to the angle θ being large, the probability for a maneuver to the other side is set to a small constant value $\alpha_{3,WP}$. The intention probabilities in (4) - (6) can be verified to sum to unity.

3) Stand-on Dependent Intention: If the obstacle is stand-on vessel in either crossing or overtaking, we assume it will be COLREGS compliant and keep its current course and speed with a constant high probability, and thus the intention probabilities for this ST are

$$\Pr\{a|B\} = \Pr\{a|C\} = \{\alpha_{1,B}, \alpha_{2,B}, \alpha_{3,B}\} \tag{8}$$

where $\alpha_{a,ST}$ for $a = 1, 2, 3$ are parameters which sum to one for any ST, and $\alpha_{a,B} = \alpha_{a,C}$ by assumption. The parameter $\alpha_{1,B}$ is typically chosen higher than 0.9 due to the COLREGS compliance assumption.

4) Give-way Dependent Intention: When the obstacle is the give-way vessel, the intention probability is assumed to follow a model dependent on the distance d_{0i}. For the overtaking situation $ST = D$, the model is assumed of the form

$$\Pr\{a = 1|D\} \propto \alpha_{1,D} e^{c_2(d_{0i} - d_{close})} \tag{9}$$

$$\Pr\{a = 2|D\} \propto (1 - \alpha_{2,D})(1 - e^{c_2(d_{0i} - d_{close})}) + \alpha_{2,D} \tag{10}$$

$$\Pr\{a = 3|D\} \propto (1 - \alpha_{3,D})(1 - e^{c_2(d_{0i} - d_{close})}) + \alpha_{3,D} \tag{11}$$

where $c_2 > 0$ is a parameter to tune the the obstacle intention a decrease/increase. For the head-on situation $ST = E$, the probabilities are assumed of the form

$$\Pr\{a = 1|E\} \propto \alpha_{1,E} e^{c_2(d_{0i} - d_{close})} \tag{12}$$

$$\Pr\{a = 2|E\} \propto (1 - \alpha_{2,E})(1 - e^{c_2(d_{0i} - d_{close})}) + \alpha_{2,E} \tag{13}$$

$$\Pr\{a = 3|E\} \propto \alpha_{3,E} \tag{14}$$

Lastly, for the crossing-on situation $ST = E$, the probabilities are assumed of the form

$$\Pr\{a = 1|F\} \propto \alpha_{1,F} e^{c_2(d_{0i} - d_{close})} \tag{15}$$

$$\Pr\{a = 2|F\} \propto (1 - \alpha_{2,F})(1 - e^{c_2(d_{0i} - d_{close})}) + \alpha_{2,F} \tag{16}$$

$$\Pr\{a = 3|F\} \propto \alpha_{3,F} \tag{17}$$

In head-on and crossing, a maneuver towards starboard will be given the highest probability, and thus $\alpha_{2,E}$ and $\alpha_{2,F}$ will be chosen higher than $\alpha_{1,E}$ and $\alpha_{1,F}$, respectively. For the overtaking case, starboard and port maneuver intentions will be given equal weight, thus $\alpha_{2,D} = \alpha_{3,D}$, also chosen higher than the weight $\alpha_{1,D}$ on keeping the current course. To avoid overconfidence in the decision of the MPC, all parameters α_{a,ST^i} are chosen strictly higher than zero. Note that only the intention of a given maneuver is quantified through these models, not the time of occurance and how much change in course and speed the maneuver will have. The intention probabilities specified in the models (9) - (11), (12) - (14) and (15) - (17) sum to one after multiplication with the inverse of the normalization constant $\sum_{a=1}^{n_a} \Pr\{a = |ST^i\}$.

This intention probability model is ad hoc, makes many assumptions and neglects a significant amount of factors. However, the point is merely to display the effect on the performance of a COLAV system when taking such information into account.

III. Obstacle Prediction Model

The obstacle motion is predicted using a stochastic OU process, as in [5], [16]. Here, the state $\boldsymbol{x}_k^i = [x_k^i, y_k^i, V_{x,k}^i, V_{y,k}^i]^T$ for obstacle i at time index k is given by the position and velocity components in north and east, respectively. The discrete time prediction model for the obstacle from time t_k to t_{k+1} can then be written as

$$\boldsymbol{x}_{k+1}^i = \boldsymbol{\Phi}(t_{k+1} - t_k, \boldsymbol{\gamma})\boldsymbol{x}_k^i + \boldsymbol{\Psi}(t_{k+1} - t_k, \boldsymbol{\gamma})\boldsymbol{v}_{OU,k}^i \tag{18}$$

where

$$\boldsymbol{\Phi}(t, \boldsymbol{\gamma}) = \begin{bmatrix} \boldsymbol{I} & (\boldsymbol{I} - e^{-\boldsymbol{\Gamma} t})\Gamma^{-1} \\ \boldsymbol{0} & e^{-\boldsymbol{\Gamma} t} \end{bmatrix} \tag{19}$$

is the transition matrix and

$$\boldsymbol{\Psi}(t, \boldsymbol{\gamma})\boldsymbol{v}_{OU,k}^i = \begin{bmatrix} t\boldsymbol{I} - (\boldsymbol{I} - e^{-\boldsymbol{\Gamma} t})\Gamma^{-1} \\ \boldsymbol{I} - e^{-\boldsymbol{\Gamma} t} \end{bmatrix} \boldsymbol{v}_{OU,k}^i \tag{20}$$

is called the control input function. The parameter $\boldsymbol{v}_{OU,k}^i$ determines typical velocities in x and y that the obstacle will tend to drift towards with time. The matrix $\boldsymbol{\Gamma}$ is chosen as $\text{diag}(\boldsymbol{\gamma})$, where $\boldsymbol{\gamma} = [\gamma_x, \gamma_y]^T$ and determines the revertion rate of the process towards the velocity $\boldsymbol{v}_{OU,k}^i$.

The covariance matrix of the predictor using the OU process can be written as

$$\boldsymbol{P}_{k+1}^i = \boldsymbol{P}_k^i + \boldsymbol{\Sigma}_1 \circ \boldsymbol{\Sigma}_2(t_{k+1} - t_k) \tag{21}$$

where $\boldsymbol{P}_k^i$ is the covariance and

$$\boldsymbol{\Sigma}_1 = \begin{bmatrix} \frac{\sigma_x^2}{\gamma_x^3} & \frac{\sigma_{xy}}{\gamma_x \gamma_y} & \frac{\sigma_x^2}{2\gamma_x^2} & \frac{2\sigma_{xy}}{\gamma_x} \\ \frac{\sigma_{xy}}{\gamma_x \gamma_y} & \frac{\sigma_y^2}{\gamma_y^3} & \frac{2\sigma_{xy}}{\gamma_y} & \frac{\sigma_y^2}{2\gamma_y^2} \\ \frac{\sigma_x^2}{2\gamma_x^2} & \frac{2\sigma_{xy}}{\gamma_y} & \frac{\sigma_x^2}{\gamma_x} & \frac{2\sigma_{xy}}{\gamma_x + \gamma_y} \\ \frac{2\sigma_{xy}}{\gamma_x} & \frac{\sigma_y^2}{2\gamma_y^2} & \frac{2\sigma_{xy}}{\gamma_x + \gamma_y} & \frac{\sigma_y^2}{\gamma_y} \end{bmatrix} \tag{22}$$

with σ_x, σ_{xy} and σ_y as the Wiener process noise parameters in the OU model. The expression for $\boldsymbol{\Sigma}_2(t_{k+1} - t_k)$ can be found in [16]. The symbol $\circ$ in (21) denotes the Hadamard product. The advantage of using this model is the limited increase in the predicted covariance, due to the revertion tendency of the process. An alternative would be to use the Constant Velocity (CV) model, which is sufficient for short-term predictions where one receive measurements frequently to reduce the uncertainty. However, for long-term predictions, the uncertainty can be overestimated by orders of magnitude when the CV model is used [5]. The model parameters in general need to be estimated depending on the ship type and the local traffic area. See [16] for more information on the OU process model derivation from the stochastic differential equation (SDE) framework.

IV. Updated Collision Probability Estimation

The work in [15] introduced a method for estimating the collision probability between the own-ship and an obstacle using the obstacle uncertainty in position and velocity in a MCS and KF scheme. The method assumes straight line trajectories for both vessels for the entire time horizon at the time of evaluation, which will be overly conservative as the vessels will most likely make maneuvers in the future to reduce collision risk. This article extends this method by calculating the collision probability on piecewise linear segments along the vessel trajectories, to reduce the conservativeness of the estimate by exploiting the intention models in Section II. A discretization time step of $T_{seg} = t_j - t_{j-1}$, for two time instants t_j and t_{j-1}, is used, typically larger than the prediction time step in the MPC. The concept is illustrated in Fig. 3 for a maneuvering own-ship and an obstacle.

Piecewise linear segments from t_{j-1} to t_j along the vessel trajectories are created, with vessel velocities given by the average over the current segment and direction along the linear segment. These segments are then used as in the original method [15] to estimate the collision probability, with one alternation: If the time until the Closest Point of Approach (CPA) t_{cpa} is less than t_j for two linear segments in consideration, the vessel states at t_j instead of t_{cpa} is used in the MCS part. This is done to constrain the collision probability evaluation to only consider positions on the discretized vessel trajectories. The obstacle covariance at the time t_{j-1} is used in the MCS [15]. This alteration naturally requires retuning of the noise parameters r_P and q_P in the estimation.

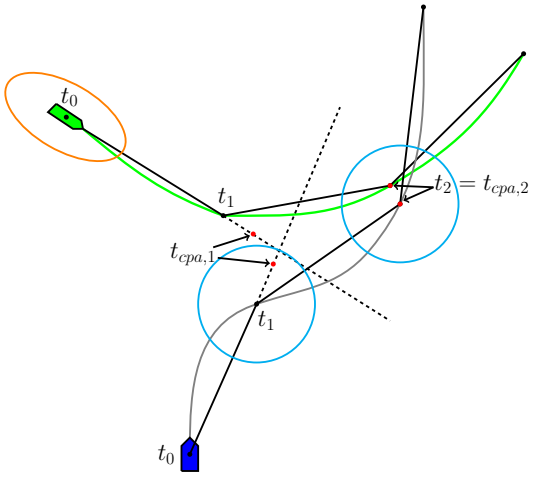

Fig. 3. Illustration of the updated collision probability estimation method. Note that T_{seg} is chosen large to make the methodology more clear. Further note that the CPA drawn in the sketch are examplatory. The obstacle (green) and own-ship (blue) trajectories are shown in green and gray, respectively. The obstacle 3σ uncertainty ellipse at t_0 is shown in orange. The black dots indicate the vessel positions at times t_0, t_1 and t_2. The red dots indicate the vessel positions along the linear segments at CPA, which for the two segments in the own-ship trajectory gives two CPA times $t_{cpa,1}$ and $t_{cpa,2}$. Since $t_{cpa,1} > t_1$, the safety zone (cyan) around the own-ship is centered to the own-ship position at t_1, where the vessel positions at t_1 is used as basis for the collision probability estimation. For the second pair of segments, $t_{cpa,2} \leq t_2$ and the safety zone is thus centered over $t_{cpa,2}$.

V. Probabilistic Scenario-Based Model Predictive Control

The PSB-MPC algorithm [15], which is an extension to the original SB-MPC [17], considers a finite set of control behaviors in the form of offsets (u_m^l, χ_m^l) to the surge u_d and course χ_d references from the ship path planner, where l is a candidate control behavior. For each control behavior, a cost function penalizing collision risk, COLREGS breaches, control reference deviation and grounding is evaluated. The optimal control behavior l^* yielding minimum cost is then selected, and the autopilot references for the autonomous ship are modified to $u_c = u_m^{l^*} \cdot u_d$ and $\chi_c = \chi_m^{l^*} + \chi_d$. See [15] for more information.

A. Enhanced Prediction Scheme

To make use of knowledge about different obstacle intentions in the MPC, the predictions must allow for port and starboard turns at different time instants in the horizon, in addition to the original straight line motion prediction. The number of turns and time of each turn for an obstacle is here determined by considering the time remaining until and distance at the estimated CPA, t_{cpa} and d_{cpa}, respectively.

If there is no predicted collision at t_{cpa}, i.e. the obstacle does not enter the safety zone of the own-ship with radius d_{safe} [15], then the alternative maneuvers are spaced evenly with t_{ts} apart throughout the horizon of length T. If there is a predicted collision, the time t_{cpa} determines how many alternative maneuvers are accounted for. Thus, the final turn time of the obstacle is given by

$$t_{ft} = \begin{cases} t_0 + T, & \text{if } d_{cpa} > d_{safe}. \\ t_0 + t_{cpa}, & \text{if } d_{cpa} \leq d_{safe} \ \& \ t_{cpa} > t_{ts}. \\ t_0, & \text{if } d_{cpa} \leq d_{safe} \ \& \ t_{cpa} \leq t_{ts}. \end{cases} \tag{23}$$

The case where $d_{cpa} \leq d_{safe}$ and $t_{cpa} > t_{ts}$ is illustrated for a head-on scenario in Figure 4. The two vessels are here predicted to collide at the blue cross (CPA).

The maneuvers are implemented by changing the velocity $\boldsymbol{v}_{OU,k}^i$ of the OU model at the turn time. In general, a finite number of different course changes can be used. In Fig. 4, three changes are used. As the explosion of obstacle uncertainty is avoided by using an OU process for prediction, its uncertainty can be divided into pieces given by the amount of different prediction scenarios specified. The spacing between turns and amount of different course changes should be set such that the union of the obstacle uncertainty in all prediction scenarios cover all possible paths. This is also a trade off with the computational effort required in the predictions.

B. Multiple Sequential Avoidance Maneuvers

To prevent conservative solutions, the PSB-MPC is allowed to make n_M sequential avoidance maneuvers in the prediction horizon. The start time of each avoidance maneuver is selected as follows. The first avoidance maneuver is made at t_0. The subsequent maneuvers are made immediately after the closest obstacle in the current collision situation makes its maneuver at $t_0 + t_{ts}$, or immediately after t_{cpa} with the closest obstacle.

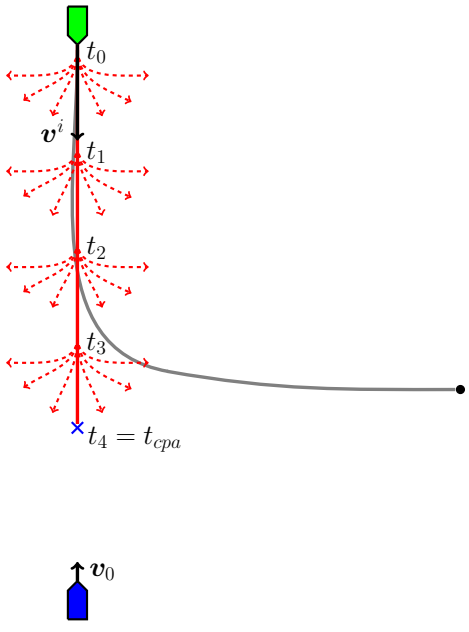

Fig. 4. The previously shown head-on scenario with obstacle i in green and own-ship (OS) in blue. Their velocity vectors $\boldsymbol{v}^i$ and $\boldsymbol{v}_0$, respectively, are also shown. The prediction scheme allows for the obstacle to make different types of port and starboard maneuvers indicated at the discrete times t_0 to t_3 in this case, in addition to the original straight line prediction. The blue cross indicates the obstacle position at t_{cpa}.

When the closest obstacle is passed, the subsequent maneuvers are found in the same manner using the next relevant close obstacle. Thus, the control behavior l now consist of the avoidance maneuvers $\left[(u^l_{m,1}, \chi^l_{m,1}), ..., (u^l_{m,n_M}, \chi^l_{m,n_M})\right]$. For the optimal control behavior l^*, the first maneuver $(u^{l^*}_{m,1}, \chi^{l^*}_{m,1})$ is the MPC output. We note that the PSB-MPC will re-evaluate its optimal strategy at regular intervals, e.g. every 5 seconds.

C. Cost Function

To account for multiple obstacle intentions and own-ship maneuvers in the prediction horizon, the PSB-MPC cost function for the own-ship control behavior l is modified to

$$\begin{aligned}\mathcal{H}^l(t_0) = &\max_i \sum_{a=1}^{n_a} \mathbb{P}^i_a(t_0) C^{l,i}_a + g(\cdot) + \\ &\frac{1}{n_M} \sum_{M=1}^{n_M} f(u^l_{m,M}, u^l_{m,M-1}, \chi^l_{m,M}, \chi^l_{m,M-1}) + \\ &\frac{1}{n_M - 1} \sum_{M=2}^{n_M} h(\chi^l_{m,M}, \chi^l_{m,M-1}, t_M - t_{M-1})\end{aligned} \tag{24}$$

where

$$C^{l,i}_a = \sum_{s=1}^{n^i_{ps}(a)} \frac{w^{i,s}}{n^i_{ps}(a)} \max_{t \in D(t_0)} \left[\mathcal{C}^{l,s}_i(t) \mathbb{P}^{l,i,s}_c(t) + \kappa_i \mu^{l,s}_i(t)\right] \tag{25}$$

is the average cost for all predicion scenarios n^i_{ps} involving intention a for obstacle i. For the case in Fig. 4, $n^i_{ps}(1) = 1$ and $n^i_{ps}(2) = n^i_{ps}(3) = 12$. The weights $w^{i,s}$ are given as

$$w^{i,s} = \begin{cases} \Pr\{CC^i\}, & \text{if obstacle } i \text{ is CC in } s \\ 1 - \Pr\{CC^i\}, & \text{otherwise} \end{cases} \tag{26}$$

The check whether the obstacle is CC in a prediction scenario is done by determining whether it breaches COLREGS given that the own-ship keeps its course. The terms $\mathcal{C}^{l,s}_i$, $\mathbb{P}^{l,i,s}_c(t)$ and $\kappa_i \mu^{l,s}_i(t)$ are the collision risk cost, collision probability and COLREGS penalization term, for control behavior sequence l, obstacle i in its prediction scenario s. Unlike [15], no discounting is made on the collision cost because this is done implicitly in the collision probability calculation when propagating the obstacle uncertainty in time. The set $D(t_0)$ contains all time samples in the prediction horizon.

The control reference cost $f(\cdot)$ is summed over all own-ship avoidance maneuvers in the control behavior l, where $u^l_{m,0} = u_{m,last}$ and $\chi^l_{m,0} = \chi_{m,last}$ are the offsets from the previous optimal MPC output. For $n_M > 1$, a new control reference cost has been introduced in $h(\cdot)$, which is given by

$$h(\chi_1, \chi_2, t) = \begin{cases} K_{sgn} e^{-\dfrac{t}{T_{sgn}}}, & \text{if sign}(\chi_1) \neq \text{sign}(\chi_2) \\ 0, & \text{otherwise} \end{cases} \tag{27}$$

and penalizes chattering behavior in course throughout the horizon, discounted by the time $t_M - t_{M-1}$ between maneuvers, with tuning parameters K_{sgn} and T_{sgn}. See [15] for more information on the cost terms and their parameters.

VI. Simulation Results

The PSB-MPC is compared against the original SB-MPC with one avoidance maneuver in two different scenarios. The performance of the PSB-MPC will be gauged when different prior probabilities on the obstacle CC is used, when it knows the next waypoint for each obstacle.

Measurements for the obstacles are generated using a covariance $\boldsymbol{R} = \text{diag}(25, 25)\text{m}^2$. Obstacles of lengths $30-100\,\text{m}$ are considered. The obstacles are initialized to the ground truth but with a single-point initialized covariance, and otherwise tracked using Kalman-filters as in [15], where the filter measurement covariance and process covariance parameters are chosen as $\boldsymbol{R}^{KF} = 2\boldsymbol{R}$ and $\sigma^{KF}_a = 0.5\,\text{m/s}^2$, respectively. This represents a conservative KF which expect fast maneuvers for the obstacle, and therefore gives higher track uncertainty, as could be the case for a real time tracking system with model mismatch and/or degraded sensor performance.

Important parameters for the SB-MPC and PSB-MPC, segment-wise collision probability estimation and intention models are summarized in Table II. The parameter d_{close} is chosen larger than in [15] because it here also determines the model switching in the ad hoc intent inference. Considering their common parameters, the two versions are tuned equally. For the PSB-MPC, course changes of 30, 60 and 90 degrees are considered for the obstacle predictions. Two sequential avoidance maneuvers are considered, where the first one samples 39 control behaviors as in [17], and the second maneuver samples a subset of those: $u_{m,2} \in \{1, 0.5\}$ and $\chi_{m,2} \in \{-90, -45, 0, 45, 90\}$ degrees, to limit the computational effort. For the MPC predictions, the initial typical velocity $\boldsymbol{v}^i_{OU,k}$ is set to the current velocity estimate of the obstacle.

Results for the two MPC versions are shown below. The own-ship using SB-MPC and PSB-MPC are shown in blue

TABLE II
Parameters for the different methods and models.

	SB-MPC	PSB-MPC
Parameter	**Value**	**Value**
r_P	-	0.001
q_P	-	0.017
T_{seg}	-	1 s
d_{close}	1000 m	1000 m
n_a	-	3
n_M	1	2
t_{ts}	-	25 s
K_{sgn}	-	5
T_{sgn}	-	$4t_{ts}$
σ_x	-	$0.8\,\text{m/s}^2$
σ_{xy}	-	$0\,\text{m/s}^2$
σ_y	-	$0.8\,\text{m/s}^2$
$\boldsymbol{\gamma}$	-	$[0.1, 0.1]^T$
$\alpha_{:,WP}$	-	$\{0.875, 0.05, 0.025\}$
$\alpha_{:,B}$	-	$\{0.9, 0.05, 0.05\}$
$\alpha_{:,D}$	-	$\{0.05, 0.475, 0.475\}$
$\alpha_{:,E}$	-	$\{0.05, 0.9, 0.05\}$
$\alpha_{:,F}$	-	$\{0.05, 0.9, 0.05\}$

and red with continuous black and dashed black trajectories, respectively. The obstacles are shown in green with their corresponding index number. The obstacle intention probabilities and distance to the obstacles are also shown. In all scenarios, the PSB-MPC knows the next waypoint for the obstacles but not their route.

In the head-on scenario in Fig. 5, the a priori CC probability is set to $\Pr\{CC^i\} = 0.1$, indicating low trust in the obstacle to follow COLREGS. The scenario is also set up such that the obstacle breaches COLREGS through a port maneuver. Due to the intent inference being used as input to the PSB-MPC, it predicts a port maneuver from the waypoint information and therefore initially slows a bit down and makes a large CC starboard maneuver. The original SB-MPC does not forsee this, and risks collision with the obstacle. This is also contributed to the uncertainty in the track estimates, which is not considered in the original SB-MPC. The switching in intent probabilities in Fig. 5b occur due to the obstacle entering the COLREGS consideration limit and when it passes the own-ship. Some oscillation in the course offset for the PSB-MPC is also seen partially due to this. Because of a small a priori CC probability, the waypoint dependent intention will dominate. Note that alternative behaviors could also be feasible, such as a port turn to minimize collision risk at the cost of breaching COLREGS. A weighting between risk aversion and COLREGS compliance must therefore be made.

Results for the same head-on scenario when having a false high trust in CC for the obstacle, by setting $\Pr\{CC^i\} = 0.9$, are shown in Fig. 6. In this case the PSB-MPC makes a smaller CC starboard maneuver, as it expects the obstacle also will act accordingly. However, as the probability of non-CC is 0.1, the waypoint dependent intent causes a higher port intention probability than the probability of keeping the current course. Thus, a more conservative starboard maneuver is made for the PSB-MPC than the SB-MPC, which gives a higher safety margin when the obstacle makes the unforseen port turn. The intention probabilities switches one time during the simulation as ST^i changes from E to A when the own-ship is passed by. As no boundary conditions are enforced on the probabilities, discrete jumps can occur. The increase in starboard turn intention at the end is due to the angle θ going positive at some point during the port turn.

Lastly, results for a combined head-on and crossing scenario are shown in Fig. 7, where a non-CC obstacle head-on to the own-ship, basically identical to the case in Fig. 5, makes a port maneuver too late, and where a CC obstacle with assumed $\Pr\{CC^2\} = 0.9$ makes a late give-way maneuver in a crossing situation. The assumed a priori CC probability for each obstacle $i = 1, 2$ is set to 0.1 and 0.9, respectively. The performance of the SB-MPC again causes large hazard with obstacle 1, as only one deterministic straight line prediction based on the current track estimates of the obstacles are considered, while the PSB-MPC is able to utilize the extra probabilistic information to make a larger proactive avoidance maneuver starboard. The algorithm could also be tuned to make the own-ship slow down and then take the turn, or make a port turn to minimize the collision risk with obstacle 1. As obstacle 2 is almost assumed fully CC, it could be safer to violate COLREGS and pass the obstacles with a port maneuver. The next waypoint for obstacle $i = 1$ again lies to the east, and the corresponding port intention dominates due to the low CC trust. Switches occur two times for the obstacles as they enter the COLREGS consideration limit and are passed by. The next waypoint for obstacle $i = 2$ lies in the south, and an increase in port intention is here seen due to the angle θ switching sign.

VII. Conclusion

The PSB-MPC extended to also consider probabilistic obstacle intentions and multiple sequential avoidance maneuvers, gives increased situational awareness and thus improved decision making. This is here shown for an ad hoc intention inference model, which is only used for illustration. As the complexity of the MPC predictions are significantly increased, further simulation studies are needed to investigate optimal tuning parameters and prediction scenario configurations. Existing methods should be used on AIS data to estimate the parameters of the OU process used in predictions. Furthermore, the robustness of the PSB-MPC for various obstacle intention probability configurations should be studied in more detail.

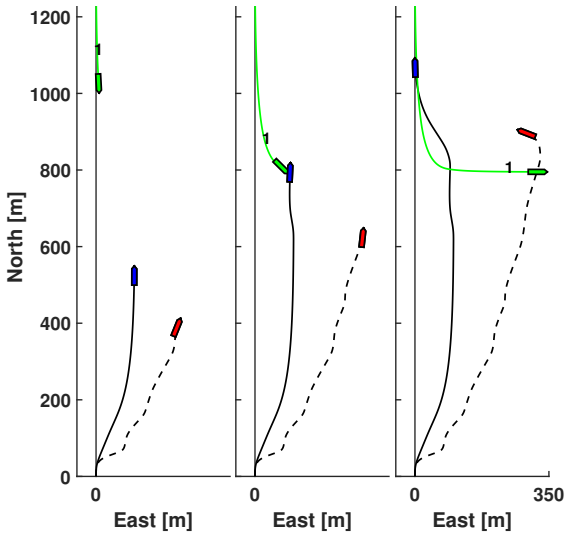

(a) North east plot at three time instants. The grey line going straight north shows the planned own-ship path.

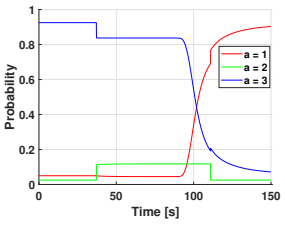

(b) Intention probabilities.

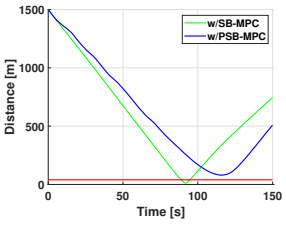

(c) Distance to obstacle with the own-ship safety zone marked as the red line.

Fig. 5. Non-CC obstacle in head-on scenario with more correct probabilistic information.

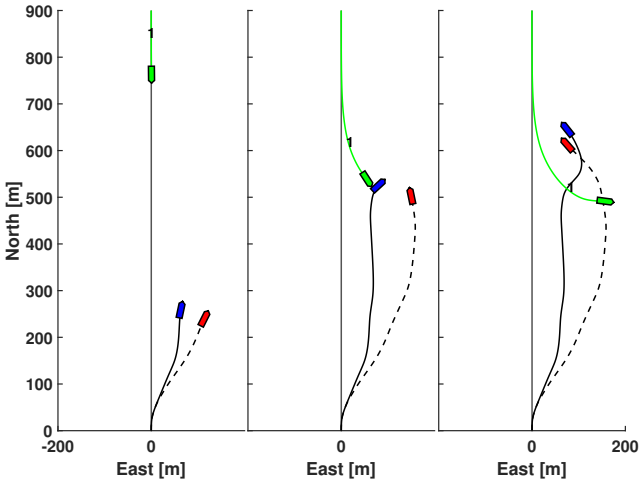

(a) North east plot at three time instants. The grey line going straight north shows the planned own-ship path.

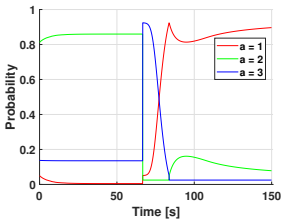

(b) Intention probabilities.

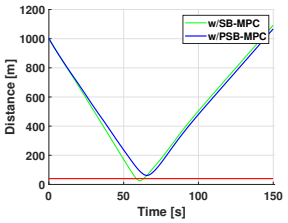

(c) Distance to obstacle with the own-ship safety zone marked as the red line.

Fig. 6. Non-CC obstacle in head-on scenario with wrong probabilistic information.

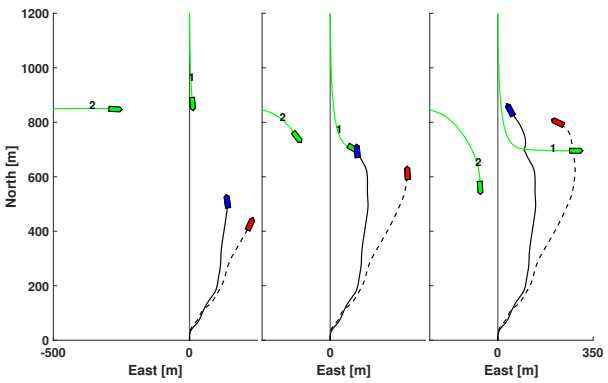

(a) North east plot at three time instants. The grey line going straight north shows the planned own-ship path.

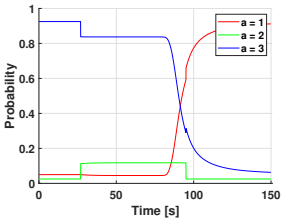

(b) Intention probabilities obstacle $i = 1$.

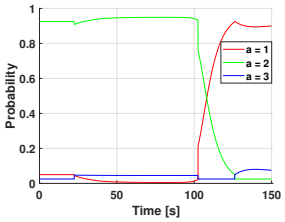

(c) Intention probabilities obstacle $i = 2$.

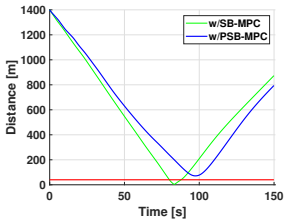

(d) Distance to obstacle $i = 1$ with the own-ship safety zone marked as the red line.

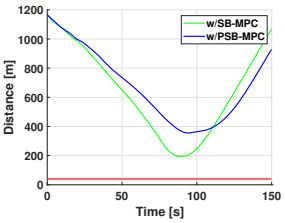

(e) Distance to obstacle $i = 2$ with the own-ship safety zone marked as the red line.

Fig. 7. Combined scenario.

REFERENCES

[1] C. Macrae, "Human factors at sea: common patterns of error in groundings and collisions," *Maritime Policy & Management*, vol. 36, no. 1, pp. 21–38, 2009.

[2] C. Chauvin, "Human factors and maritime safety," *Journal of Navigation*, vol. 64, pp. 625 – 632, 10 2011.

[3] O. Levander, "Autonomous ships on the high seas," *IEEE Spectrum*, vol. 54, no. 2, pp. 26–31, February 2017.

[4] C. Paris, "Norway takes lead in race to build autonomous cargo ships," Jul. 2017. [Online]. Available: https://www.wsj.com/articles/norway-takes-lead-in-race-to-build-autonomous-cargo-ships-1500721202

[5] L. M. Millefiori, P. Braca, K. Bryan, and P. Willett, "Long-term vessel kinematics prediction exploiting mean-reverting processes," in *2016 19th International Conference on Information Fusion (FUSION)*, July 2016, pp. 232–239.

[6] S. Hexeberg, A. L. Flaten, B.-O. H. Eriksen, and E. F. Brekke, "Ais-based vessel trajectory prediction," *20th International Conference on Information Fusion*, pp. 1–8, 2017.

[7] B. R. Dalsnes, S. Hexeberg, A. L. Flaten, B.-O. H. Eriksen, and E. F. Brekke, "The neighbor course distribution method with gaussian mixture models for ais-based vessel trajectory prediction," *21st International Conference on Information Fusion*, pp. 580–587, 2018.

[8] E. Tu, G. Zhang, S. Mao, L. Rachmawati, and G. Huang, "Modeling historical ais data for vessel path prediction: A comprehensive treatment," *ArXiv*, vol. abs/2001.01592, 2020.

[9] B. Ahmad, J. Murphy, P. Langdon, and S. Godsill, "Bayesian intent prediction in object tracking using bridging distributions," *IEEE Transactions on Cybernetics*, vol. 48, pp. 215 – 227, 01 2018.

[10] I. Hwang and C. E. Seah, "Intent-based probabilistic conflict detection for the next generation air transportation system," *Proceedings of the IEEE*, vol. 96, no. 12, pp. 2040–2059, Dec 2008.

[11] J. Hardy and M. Campbell, "Contingency planning over probabilistic obstacle predictions for autonomous road vehicles," *IEEE Transactions on Robotics*, vol. 29, no. 4, pp. 913–929, Aug. 2013.

[12] B. C. Shah, P. Švec, I. R. Bertaska, A. J. Sinisterra, W. Klinger, K. von Ellenrieder, M. Dhanak, and S. K. Gupta, "Resolution-adaptive risk-aware trajectory planning for surface vehicles operating in congested civilian traffic," *Autonomous Robots*, vol. 40, no. 7, pp. 1139–1163, 2016.

[13] Y. Cho and J. Kim, "Collision probability assessment between surface ships considering maneuver intentions," in *Proc. OCEANS 2017 - Aberdeen*, Jun. 2017, pp. 1–5.

[14] IMO, "COLREGS - International Regulations for Preventing Collisions at Sea," *Convention on the International Regulations for Preventing Collisions at Sea, 1972*, 1972.

[15] T. Tengesdal, E. F. Brekke, and T. A. Johansen, "On collision risk assessment for autonomous ships using scenario-based-MPC," *IFAC World Congress, Berlin*, 2020, in press.

[16] L. Millefiori, P. Braca, K. Bryan, and P. Willett, "Modeling vessel kinematics using a stochastic mean-reverting process for long-term prediction," *IEEE Transactions on Aerospace and Electronic Systems*, vol. 52, 10 2016.

[17] T. A. Johansen, T. Perez, and A. Cristofaro, "Ship collision avoidance and COLREGS compliance using simulation-based control behavior selection with predictive hazard assessment," *IEEE Transactions on Intelligent Transportation Systems*, vol. 17, no. 12, pp. 3407–3422, Dec. 2016.